Deformation behavior of a modified 5083 aluminum alloy

R. Kaibyshev[a,*], F. Musin[a], E. Avtokratova[a], Y. Motohashi[b]

[a] *Institute for Metals Superplasticity Problems RAS, Khalturina 39, Ufa 450001, Russia*
[b] *Ibaraki University, The Research Center for Superplasticity, Hitachi, Ibaraki, Japan*

Abstract

The deformation behavior of a 0.2% Zr and 1.6% Mn modified 5083 aluminum alloy was studied in the temperature range of 250–570 °C over seven orders of magnitude of strain rates. It was shown that the modified 5083 alloy exhibits threshold behavior in the temperature interval of 250–500 °C. There exists a temperature dependence of threshold stress with the energy term $Q_0 = 18$ kJ/mol. It was shown by transmission election microscopy that detachment of dislocations from dispersoids under extra force takes place. Threshold stress tends to disappear with increasing temperature at $T > 500$ °C despite the fact that evidence for interactions between mobile dislocations and dispersoids was found at these temperatures. Analysis of creep data in terms of threshold stress revealed three different types of deformation behavior. At high values of normalized strain rate, $\dot{\varepsilon}kT/(D_1Gb) > 4 \times 10^{-8}$, the exponential law creep takes place. At normalized strain rates, $\dot{\varepsilon}kT/(D_1Gb)$, ranging from 4×10^{-8} to 4×10^{-14}, the n value is ~4 and the true activation energy, Q_c, is equal to 139 ± 12 kJ/mol, suggesting high temperature dislocation climb. At low normalized strain rate, a transition to Newtonian viscous flow occurs.

Keywords: Creep; Deformation mechanism; Al–Mg alloy; Threshold stress; Dispersoids

1. Introduction

It is known that aluminum alloys containing unshearable dispersoids normally exhibit a superior creep resistance at elevated temperatures due to the presence of a threshold stress, below which the strain rate is assumed to be negligible [1–12].

Threshold behavior of dispersion-strengthened aluminum alloys is originated from very fine particles impeding the motion of lattice dislocations [3–8]. In the aluminum alloys and discontinuous aluminum matrix composites produced by powder metallurgy (PM) these dispersoids can be oxides resulted from the technological route [4,5–7]. These oxides serve as effective barriers to dislocation motion and give rise to the threshold stress for creep [4–11]. As a result, the creep strain rate in these materials is essentially lower than that in solid solution aluminum alloys produced by ingot metallurgy (IM) at similar values of temperature and applied stress. At the same time, the IM aluminum alloys are attractive materials for high temperature applications due to good combination of creep resistance, strength, and fracture toughness [12].

Recently, it has been demonstrated that IM aluminum based composite [13,14] as well as aluminum alloys [15] can also exhibit threshold behavior. However, at present the origin of the threshold stress in these materials is under discussion. In a previous work [15] it was shown that an ingot metallurgy (IM) 2219 aluminum alloy exhibits threshold behavior. The values of threshold stress in this material and in two PM Al–Cu–Mg–Mn alloys [7,9] were found to be essentially the same. Therefore, it can be expected that fine second-phase particles of transition elements can play a similar role in IM aluminum alloys enhancing their creep resistance at high temperature deformation as nanoscale oxides in PM aluminum alloys.

The present work aims to provide detailed information on the deformation behavior of an 5083 aluminum alloy additionally alloyed by 0.2 wt.% Zr. This material produced by

* Corresponding author. fax: +7 3472 253759.
E-mail address: rustam@anrb.ru (R. Kaibyshev).

ingot metallurgy contains dispersoids of Al_3Cr and Al_3Zr [16] and, therefore, can exhibit threshold behavior.

2. Experimental material and procedures

An experimental version of the 5083 aluminum alloy, denoted as 5083 Al herein, with a chemical composition Al–4.7% Mg–1.6% Mn–0.2% Zr–0.18% Cr–0.1% Fe (in wt.%) was manufactured at Kaiser Aluminum and Chemical Corporation, Pleasanton, CA, USA. The alloy was fabricated by direct chill casting and homogenized at 520 °C for 10 h.

Full details of two types of mechanical tests used in the present study were given earlier [15,17]. In the present investigation, the compression tests were conducted in the temperature range 250–570 °C at strain rates ranging from 1.4×10^{-6} to $6 \times 10^{-2}\,s^{-1}$. A Schenk RMS-100 universal testing machine was used. In order to obtain additional experimental points at low strain rates in the temperature range 250–300 °C, creep tests were carried out at constant stress in tension using a creep machine with a contoured Andrade–Chalmers lever arm. In these experiments, the resultant steady-state creep rates ranged from 1.2×10^{-8} to $1.2 \times 10^{-4}\,s^{-1}$.

Specimens of 10 mm in diameter and 12 mm in height for the compression test and specimens of 20 mm in gauge length and 5 mm in diameter for the tension test were machined from the ingot. Both tests were conducted in air using a furnace in which the temperature was monitored and maintained constant within ±2 K. Each sample was held at a testing temperature for about 30 min in order to reach thermal equilibrium.

The microstructure of the material tested in the present study was examined by means of transmission electron microscopy (TEM) technique which was described in details in recent work [16]. Samples for TEM study were cut from the cross section of specimens, which were quenched in water in a furnace immediately after deformation.

3. Experimental results

3.1. Mechanical behavior

Typical true stress–true strain curves are shown in Fig. 1 for temperatures ranging from 250 to 570 °C. The σ–ε curves, which are representative for all testing conditions, exhibit a well-defined steady-state flow after a very short transient stage of plastic deformation ($\varepsilon < 0.1$).

Fig. 2 shows a plot of the steady state creep rate against strain obtained from the uninterrupted test (curve I) and the stress-change test (curve II). It is seen that the creep curve I also exhibits a very short stage of primary creep. Steady-state flow was attained at true strain values over 0.004. During the stress change tests a new steady-state was achieved after a very short transient stage (Fig. 2, curve II).

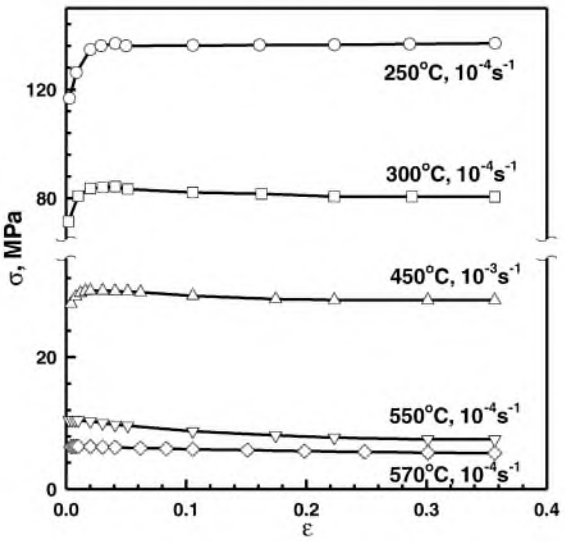

Fig. 1. True stress–true strain curves for the 5083 Al.

Note the data obtained from the uninterrupted tests show good agreement with those obtained from interrupted tests both in compression and in tension experiments as well.

3.2. Stress dependence of steady-state strain rates

Fig. 3 shows the variation of the imposed strain rate with the steady-state stress for Schenk test and the dependence of the steady-state creep rate on the applied stress for creep test on a double logarithmic scale, for temperatures ranging from 250 to 570 °C. One can see that the data obtained from the Schenk test show excellent agreement with those obtained from creep machine tests. Three temperature–strain regions

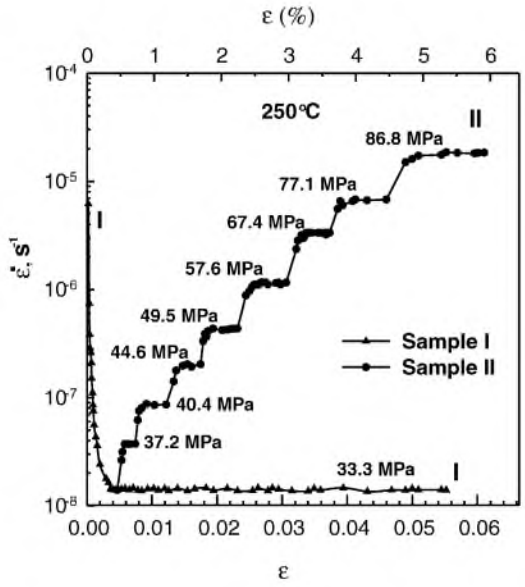

Fig. 2. Example of stress increase experiments and a creep curve for the 5083 Al.

can be distinguished, according to a change of the apparent stress exponent, n_a, with decreasing strain rate.

At $\sigma > 100$–130 MPa (high stress region), the n_a value tends to decrease from ~26 to ~7 with decreasing strain rate suggesting that the deformation behavior in this region can be equivalently represented by an exponential relationship [1,2,18,19]:

$$\dot{\varepsilon} = B \exp(\beta\sigma) \exp\left(\frac{-Q}{RT}\right), \quad (1)$$

where $\dot{\varepsilon}$ is the strain rate, B is a constant, β is a coefficient, σ is steady state flow stress, Q is the activation energy for plastic deformation, R is the gas constant and T is the absolute temperature [1,2,18,19]. To confirm the validity of Eq. (1), the datum point in the high stress region were plotted in a semi-logarithmic scale. It was found that this plot provides the best linear fit with a regression coefficient of 0.98.

In the intermediate stress region ($4 < \sigma < 100$–130 MPa), the best fit to the experimental data is given by a power law relationship of the usual form:

$$\dot{\varepsilon} = A\sigma^n \exp\left(\frac{-Q}{RT}\right), \quad (2)$$

where A is a constant and n_a is the stress exponent. At $T = 250$ °C, the apparent stress exponent increases from ~5 at ~80 MPa to ~9 at ~30 MPa, at 450 °C, the n_a value increases from ~5 to ~7 when the applied stress decreases from ~50 to ~9 MPa. This creep behavior of the modified 5083 Al resembles that of dispersion-strengthened alloys [4–11]. Generally, in this stress region, a temperature increase results in decreasing the stress exponent. Notably, the transition from high stress region to intermediate stress region occurs at stress about 100–130 MPa, which are slightly higher than that for the dilute Al–5% Mg alloy [19].

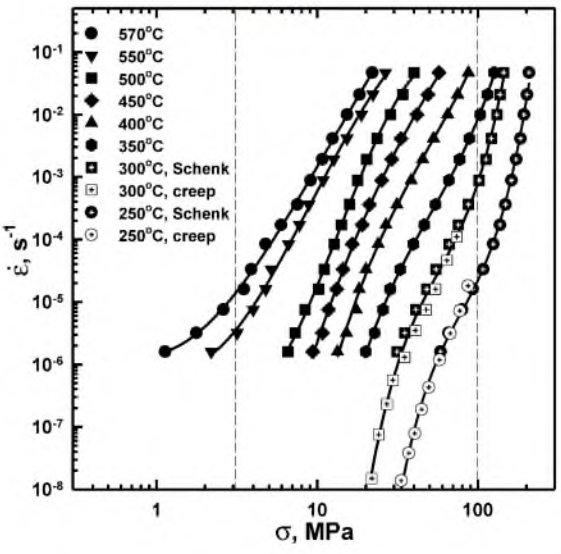

Fig. 3. Plot of strain rate vs. steady state flow stress on logarithmic scale. Broken lines deviates the intermediate stress region from low stress region and high stress region.

At $T \geq 550$ °C, two different types of deformation behavior of the 5083 Al can be distinguished (Fig. 3). In the intermediate stress region, the value of apparent stress exponent is essentially constant (~4). In the low stress region $\sigma < 4$ MPa at $T \geq 550$ °C, the n_a value tends to decrease from 4.0 to 1.5 with decreasing stress approaching to ~1.

3.3. Temperature dependence of steady-state stress

The apparent activation energy of plastic deformation, Q_a, was computed through a procedure described in works [15,17,20] in details. Algebraically, Eq. (2) can be converted to

$$\ln \sigma_o = A^* + \frac{Q}{nR} \times \frac{1}{T}, \quad (3)$$

where $A^* = \ln(A^{-1/n}\dot{\varepsilon}^{1/n})$ is a constant, taking into account that datum point at a fixed strain rate were used. The Q_a values were obtained by the plotting of the modulus-normalized stress, σ/G, using the temperature dependence of shear modulus for pure Al (in MPa) defined as [13,14]:

$$G = (3.022 \times 10^4) - 16T, \quad (4)$$

against the inverse of the absolute temperature logarithmically [15,17,20] for different values of strain rate. The slope of this dependence is equal to $Q_a/(nR)$ [15,17,20]. It was found that the values of apparent activation energy ranging from 176 ± 30 to 470 ± 120 kJ/mol are appreciably higher than the activation energy for lattice self-diffusion in pure Al ($Q_l = 143.4$ kJ/mol [21]), that can be attributed to existence of the threshold stress [4,5,7,8].

3.4. Microstructure observation

Following solution treatment, TEM study revealed the presence of small particles identified as Al_3Cr, Al_3Zr and Al_6Mn by energy dispersive spectroscopy technique in the previous work [16]. These dispersoides located quite uniformly within the grain interior. TEM observations showed that the other secondary phases did not precipitate during deformation at all temperatures. The microstructure of the starting material consists of equiaxed grains with an average size of ~180 μm; average dislocation density was ~10^{11} m^{-2}.

TEM observations of strained samples revealed an extensive interaction between dislocations and second-phase particles (Fig. 4). Lattice dislocations attach to small particles, climb over them and are captured at the detachment side of the particles after the climb has been completed (Fig. 4a). At $T \geq 550$ °C, the lattice dislocations climbing over particles usually exhibit a weaker dislocation curvature (Fig. 4b). It was recently shown [22] that this dislocation configuration suggests the occurrence of dislocation glide along the matrix-particle interface readily under applied stress, and does not require an extra force. However, they are strongly captured at the detachment side of the particles (Fig. 4a) indicating a high interaction force at these temperatures [22].

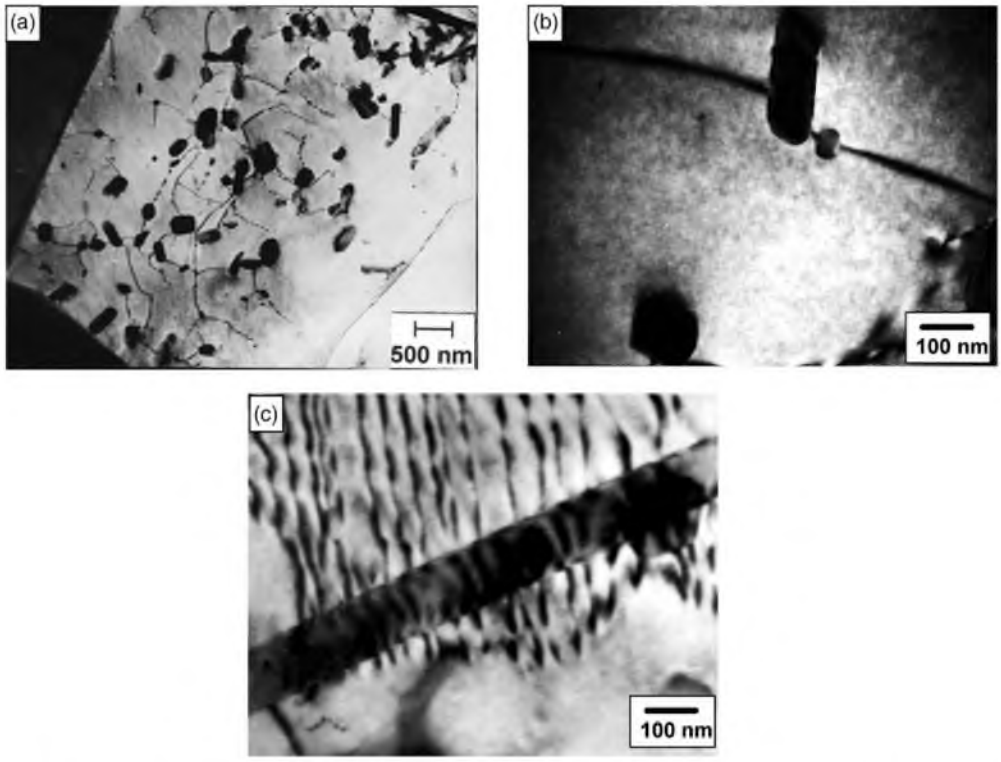

Fig. 4. TEM observation of the 5083 Al strained up to a true strain of 2.3 at $\dot{\varepsilon} = 10^{-3}\,s^{-1}$: (a, b) $T = 570\,^{\circ}C$, (c) $T = 450\,^{\circ}C$.

An evidence for strong attractive dislocation–dispersoid interaction was found at the interface boundaries between the matrix and the Al_6Mn particles (Fig. 4c). A specific diffraction contrast, which is indicative for dissociation of lattice dislocations on grain boundary dislocations (GBD) at the interfaces [23,24], is observed on a dislocation segment placing on a plane of an interface boundary (Fig. 4c). This interaction process is essentially similar to the dissociation of lattice dislocations into extrinsic GBDs at elevated temperatures ($T > 0.4\,T_m$, where T_m is melting point) followed by their adsorption [24]. Increasing temperature leads to elimination of diffraction contrast from a lattice dislocation at the interface boundary (Fig. 4b) suggesting a deep relaxation of the elastic stress originated from the bypassing dislocations.

4. Analysis and discussion

Inspection of the deformation behavior shows that the 5083 Al exhibits threshold behavior in the intermediate stress region. Data of TEM observation obviously support this conclusion. Therefore, the deformation behavior of the 5083 Al alloy can be represented by an equation accounting for the threshold stress, σ_o [1–8]:

$$\dot{\varepsilon} = A\left(\frac{\sigma - \sigma_o}{G}\right)^n \exp\left(\frac{-Q}{RT}\right), \tag{5}$$

4.1. Examination of the presence of a threshold stress

The threshold stress was estimated using datum points from the intermediate stress region (Fig. 3). The datum points lying above the Sherby–Burke criterion representing the breakdown of power-law creep [18]:

$$\frac{\dot{\varepsilon}}{D} = 10^{13}\,m^{-2}, \tag{6}$$

where D_l is the lattice self-diffusion coefficient in pure Al calculated as [13,21]:

$$D = 1.86 \times 10^{-4} \exp\left(\frac{-143.4 \times 10^3}{RT}\right), \; m^2/s. \tag{7}$$

were discarded. In the temperature range 550–570 °C the datum points for which $\sigma \geq 4$ MPa were taken into account to estimate the magnitude of the threshold stress.

A standard procedure was used to determine the threshold stress [1–7]. The experimental data at a single temperature were plotted as $\dot{\varepsilon}^{1/n}$ against the steady state flow stress, σ, on a double-linear scale. The datum points of this plot were best fitted a straight line by varying the n values. The n values were taken as 2, 3, 4, 5, 7. The stress exponent of 4 yields the best fit between $\dot{\varepsilon}^{1/n}$ and σ. It is worth noting that for $n = 3$ representing the process of viscous dislocation glide [25–28] the data of the plots exhibit well-defined curvature that rules out the process of viscous glide of dislocation in an atmosphere of solute atoms [27,28] as the rate-controlling process.

Table 1
Threshold stress at different temperatures

T(°C)	σ_o, (MPa)
250	20.1
300	13.3
350	9.9
400	8.5
450	5.5
500	3.9
550	0.58
570	0.03

The threshold stresses at different temperatures are summarized in Table 1. It is seen that in the temperature range 250–500 °C the values of threshold stress range from 20.1 to 3.9 MPa. At $T \geq 550$ °C, the σ_o values become very low suggesting the disappearance of the threshold stress at high testing temperatures. This is why the value of the apparent stress exponent $n_a \sim 4$ (see Fig. 3) matches with the true stress exponent value inferred from the present analysis with high accuracy.

Fig. 5 represents the temperature dependence of the normalized threshold stress which can be expressed by a relationship of the form [1–8]:

$$\frac{\sigma_o}{G} = B_o \exp\left(\frac{Q_o}{RT}\right), \tag{8}$$

where B_o is a constant and Q_o is an energy term representing the activation energy for a dislocation to overcome an obstacle. In the temperature range 250–500 °C the value of Q_o inferred from the slope of this plot is ~18 kJ/mol. This value is close to the Q_o values reported for PM aluminum alloys [5,7,9].

4.2. The origin of the threshold stress

The preceding analysis shows that the present 5083 Al behaves like a dispersion strengthened aluminum alloy. The origin of the threshold stress is attributed to the presence of Al_3Zr, Al_3Cr and Al_6Mn incoherent particles. TEM observations clearly confirmed the existence of a strong attractive interaction between particles and mobile lattice dislocations (Fig. 4). The stable incoherent particles are bypassed by a sequential process consisting of local climb, glide of climbing portion of lattice dislocation along interface boundary and subsequent detachment [29–32]. However, the strong dependence of the normalized threshold stress on temperature (Fig. 5) clearly rules out the three well-known models developed to explain the magnitude of threshold stress [4–7]. In these models, the threshold stress is equal to stress required: (a) to bow a dislocation between two particles (Orowan stress) [1], (b) to create the additional dislocation segment as a dislocation surmounts an obstacle by local climb [33,34], (c) to detach a dislocation from an attractive particle after climb is completed [29–32]. All these theoretical models predict the threshold stress being independent on temperature. A recent theoretical model [35] predicts the existence of a weak temperature dependence of the threshold stress. However, this model was based on assumptions of extensive nucleation and separation of a jog pair along a climbing dislocation and no attractive particle–dislocation interaction that is inconsistent with TEM data. Thus, nowadays there are no theoretical models which can be used to explain the origin of threshold stress in the 5083 Al.

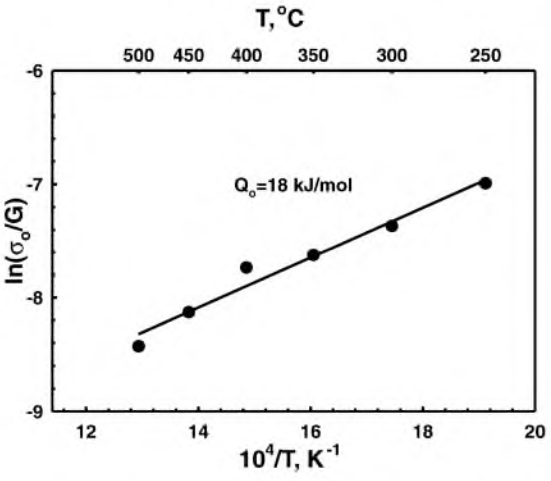

Fig. 5. Plot of the logarithm of the normalized threshold stresses vs. the inverse of the absolute temperature.

Comparing the temperature dependence of threshold stress with TEM data we can conclude that a decrease in threshold stress associates with the lowering of the dislocation energy at the matrix-particle interface resulted from dissociation of the climbing segment of this dislocation into interfacial dislocations. It is worth noting that this lowering has to increase the threshold stress originated from detachment process [29–32]; TEM observations confirmed the existence of a high extra force to detach a dislocation from a dispersoid at $T \geq 550$ °C (Fig.4a). The disappearance of the threshold stress near melting temperature reported recently for numerous aluminum alloys and metal matrix composite [36–38] in the 5083 Al correlates with the disappearance of extra force which is required for dislocation glide along matrix-particle interfaces in the temperature range in which the true threshold stress exists.

4.3. True activation energy

The aforementioned procedure was applied to determine the true activation energy; the normalized effective stresses $((\sigma-\sigma_{th})/G)$ for the intermediate stress region were plotted as a function of $1/T$ on semi-logarithmic scale at a fixed strain rate (Fig. 6). Values of the true activation energy, Q_c, were computed assuming that Eq. (5) adequately describes the deformation behavior of the present 5083 Al. It is seen that Q_c value is about 139 ± 12 kJ/mol that is very similar to the activation energy for lattice self-diffusion in Al (143.4 kJ/mol [21]). Thus, the incorporation of a threshold stress in the ac-

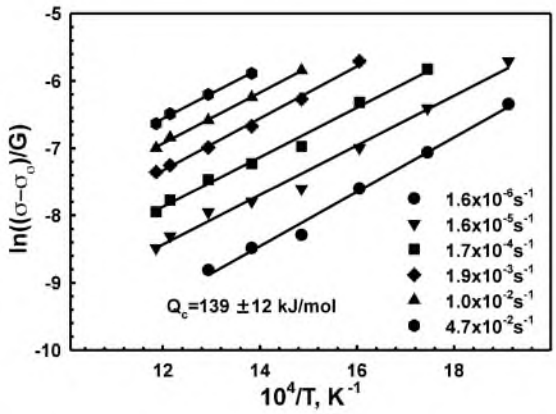

Fig. 6. Shear modulus compensated effective stress vs. the inverse of the absolute temperature.

tivation energy analysis provides realistic values of the true activation energy.

4.4. An examination of the normalized creep data

Fig. 7 represents a double logarithmic plot of the normalized strain rate, $\dot{\varepsilon}kT/(D_l Gb)$, against the normalized effective stress, $(\sigma-\sigma_0)/G$. The Burgers vector $b=2.86\times10^{-10}$ m and the lattice diffusion coefficient, D_l, were taken for pure Al [14]. The Sherby–Burke criterion [18] of $\dot{\varepsilon}/D < 10^{13}\ \mathrm{m}^{-2}$ representing the breakdown of power-law creep, is indicated in Fig. 7 for the upper and lower testing temperatures of 250 and 570 °C. The 5083 Al exhibits a well-defined power-law relationship with the stress exponent $n\sim4.15$ at the normalized strain rates ranging from 4×10^{-8} to 4×10^{-14}. This value of the stress exponent and the value true activation energy being similar to the activation energy for self-diffusion in pure Al suggest that a high-temperature dislocation climb

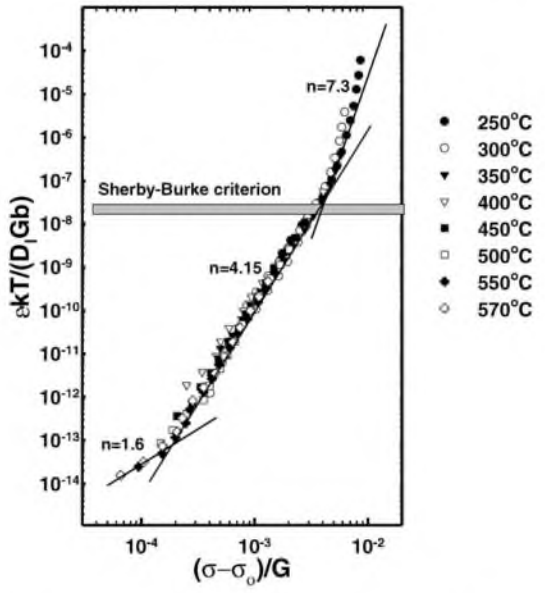

Fig. 7. Normalized strain rate vs. normalized stress for the 5083 Al.

controlled by vacancy diffusion through the lattice is the rate-controlling mechanism at these conditions. Data points giving $n>7$ lie above Sherby–Burke criterion for power-law breakdown. It was shown [19] that the deformation behavior described by exponential-law with $n\sim7$ in an Al–5% Mg could be equally represented by Eq. (1). Therefore, it is apparent that the data points lying above the Sherby–Burke criterion represent exponential creep regime.

At the lowest normalized strain rate $\dot{\varepsilon}kT/(D_l Gb) < 4\times10^{-14}$, the stress exponent is equal to ~1.4. At these conditions, there exists a likelihood for transition from dislocation creep controlled by high temperature climb with $n=4.15$ to Newtonian viscous flow with $n=1.0$ suggesting the occurrence of diffusion creep [1,2] or Harper–Dorn creep [39–41] in low stress region. Thus, the creep behavior of the 5083 Al divides into three different classes: exponential low creep, high temperature dislocation creep and Newtonian viscous flow. In comparison with Al–5% Mg alloy [25,42] no evidence for viscous glide-controlled creep in the 5083 Al was revealed.

4.5. An effect of transition elements on deformation behavior of Al–5% Mg alloy

Comparing data on creep behavior of dilute Al–5% Mg alloys reported previously [19,25,43] and obtained in the present study it is possible to conclude that the introducing of Mn, Cr and Zr into Al–5% Mg alloy resulted in an enhancement of creep resistance of this material (Fig. 8). This strengthening is caused by two factors.

(i) It is known [21,44] that near melting temperature the additions of ~0.4% Mn into pure aluminum results in a decrease in the interdiffusion coefficient by a factor of 10. By analogy, one may assume that the introducing of Mn,

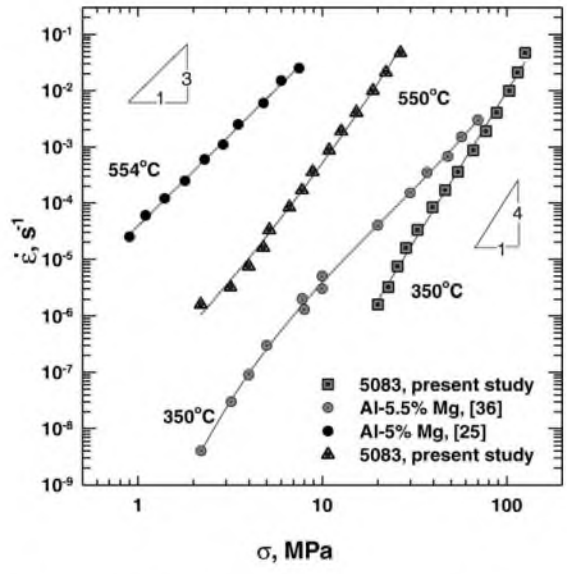

Fig. 8. Creep strengthening of Al–5% Mg solid solution by adding 1.6% Mn, 0.18% Cr and 0.2% Zr.

Cr and Zr into the Al–Mg solid solution hinders lattice diffusion and, therefore, decrease the rate of dislocation climb.

(ii) The formation of Al_6Mn, Al_3Cr and Al_3Zr dispersoids [17] provides the strengthening due to arising threshold stress.

It is apparent that the first factor provides the enhancement of creep strength suppressing viscous dislocation glide at $T \geq 550\,^{\circ}C$ (Fig. 8). The dispersion strengthening gives a significant contribution into creep resistance at $T \leq 350\,^{\circ}C$ and low strain rates. Thus, the introducing of transition elements is an attractive way to enhance creep resistance of Al alloys.

5. Conclusion

(i) The deformation behavior of the 0.2% Zr and 1.6% Mn modified 5083 Al was examined at temperatures ranging from 250 to 570 °C in the strain rate range from 2×10^{-8} to $6 \times 10^{-2}\,s^{-1}$. Analysis of experimental data of the 5083 Al revealed the presence of a threshold stress in the temperature range 250–500 °C in which the threshold stress depends on temperature with an energy term, Q_o, of 18 kJ/mol. At $T > 500\,^{\circ}C$, the disappearance of the threshold stress takes place.

(ii) By incorporating the threshold stress into the analysis, it was shown that at the normalized strain rates $\dot{\varepsilon}kT/(D_1Eb)$ ranging from 4×10^{-8} to 4×10^{-14} the true stress exponent value n is ~4 and the true activation energy, Q_c, is 139 ± 12 kJ/mol. At higher normalized strain rate, the n value is ~7.3 and Q_c value tends to decrease. At lower normalized strain rate, the n value is ~1.4.

(iii) A detachment of lattice dislocations from dispersoids under extra force was found at all temperatures examined including the temperature interval 550–570 °C where the threshold stress disappears. Extensive dissociation of bypassing segments of lattice dislocations on grain boundary dislocations (GBD) at the matrix–particle interfaces occurs.

References

[1] J. Čadek, Creep in Metallic Materials, Academia, Prague, 1994, p. 302.
[2] R.W. Evans, B. Wilshire, Creep of Metals and Alloys, The Institute of Metals, London, 1985, p. 314.
[3] D.C. Dunand, A.M. Jansen, Acta Mater. 45 (1997) 4569.
[4] F.A. Mohamed, K.T. Park, E.J. Lavernia, Mater. Sci. Eng. A 150 (1992) 21.
[5] K.T. Park, E. Lavernia, F. Mohamed, Acta Metall. Mater. 42 (1994) 667.
[6] Y. Li, S.R. Nutt, F. Mohamed, Acta Mater. 45 (1997) 2607.
[7] Y. Li, F.A. Mohamed, Acta Mater. 45 (1997) 4775.
[8] L. Kloc, S. Spigarelli, E. Cerri, E. Evangelista, T.G. Langdon, Acta Mater. 45 (1997) 529.
[9] J. Čadek, S.J. Zhu, K. Milicka, Mater Sci. Eng. A 248 (1998) 65.
[10] J. Čadek, S.J. Zhu, K. Milicka, Mater Sci. Eng. A 252 (1998) 1.
[11] J. Čadek, K. Kucharova, S.J. Zhu, Mater Sci. Eng. A 281 (2000) 162.
[12] J.S. Robinson, R.L. Cudd, J.T. Evans, Mater. Sci. Technol. 19 (2003) 143.
[13] Y. Li, T.G. Langdon, Acta Mater. 45 (1997) 4797.
[14] Y. Li, T.G. Langdon, Acta Mater. 46 (1998) 1143.
[15] R. Kaibyshev, O. Sitdikov, I. Mazurina, D.R. Lesuer, Mater. Sci. Eng. A 334 (2002) 104.
[16] R. Kaibyshev, F. Musin, D.R. Lesuer, T.G. Nieh, Mater. Sci. Eng. A 342 (2003) 169.
[17] R. Kaibyshev, I. Kazakulov, Mater. Sci. Tech. 20 (2004) 221.
[18] O.D. Sherby, P.M. Burke, Progr. Mater. Sci. 13 (1967) 325.
[19] M.R. Drury, F.J. Humphreys, Acta Metall. 34 (1986) 2259.
[20] J.R. Pickens, T.J. Langan, R.O. England, M. Liebson, Metall. Trans. 18A (1987) 303.
[21] Landolt-Bornstein, Numerical Data and Functional Relationships in Science and Technology, New Series, Group III: Crystals and Solid State Physics. Diffusion in solid Metals and Alloys, 26, 1990, pp.60 and 151.
[22] D. Haussler, M. Bartsch, U. Messerschmidt, B. Reppich, Acta Mater. 49 (2001) 3647.
[23] R.C. Pond, D.A. Smith, Phil. Mag. 36 (1977) 353.
[24] R.Z. Valiev, V.Yu. Gertsman, O.A. Kaibyshev, Phys. Stat. Sol. (a) 97 (1986) 11.
[25] P. Yavari, F. Mohamed, T.G. Langdon, Acta Metall. 29 (1981) 1495.
[26] P. Yavari, T.G. Langdon, Acta Metall. 30 (1982) 2181.
[27] H. Oikawa, T.G. Langdon, in: B. Wilshire, R.W. Evans (Eds.), Creep behavior of Crystalline Solids, Pineridge Press, UK, 1985, p. 63.
[28] H. Oikawa, et al., Scr. Metall. 10 (1976) 885.
[29] E. Arzt, D.S. Wilkinson, Acta Metall. 34 (1986) 1893.
[30] E. Arzt, J. Rösler, Acta Metall. 36 (1988) 1053.
[31] B. Reppich, Acta Mater. 46 (1998) 61.
[32] J. Rossler, E. Arzt, Acta Metall. Mater. 38 (1990) 671.
[33] E. Arzt, M.F. Ashby, Scr. Metall. 16 (1982) 1285.
[34] J. Rosler, E. Arzt, Acta Metall. 36 (1988) 1043.
[35] A. Pichler, E. Arzt, Acta Mater. 44 (1996) 2751.
[36] J. Čadek, K. Kucharova, S.J. Zhu, Mater. Sci. Eng. A 272 (1999) 45.
[37] J. Čadek, K. Kucharova, S.J. Zhu, Mater. Sci. Eng. A 283 (2000) 172.
[38] K. Kucharova, I. Saxl, J. Cadek, Acta Metall. 22 (1974) 465.
[39] J. Harper, J.E. Dorn, Acta Metall. 5 (1957) 654.
[40] C.R. Barrett, E.C. Muehleisen, W.D. Nix, Mater. Sci. Eng. 10 (1972) 33.
[41] F.A. Mohamed, K.L. Murty, J.W. Morris, Metall. Trans. 4 (1973) 935.
[42] M. Pahutova, J. Čadek, Phys., Stat. Sol. (a) 56 (1979) 305.
[43] K. Kucharova, I. Saxl, J. Cadek, Acta Metall. 22 (1974) 465.
[44] H. Buckle, Z. Electrochem. 49 (1943) 238.